

BELLCOMM, INC.

955 L'ENFANT PLAZA NORTH, S.W.

WASHINGTON, D.C. 20024

B70 09070

SUBJECT: Generalization of the Skylab
Orbital Workshop Thermal Model
to Accept Transient External
Absorbed Heat Input Data
Case 620

DATE: September 28, 1970
FROM: D. P. Woodard
A. W. Zachar

ABSTRACT

The MSFC/S&E-ASTN Orbital Workshop thermal model (MOWS) has been generalized to accept transient external absorbed heat input data. This generalization considerably extends the capability of the MOWS by permitting the use of time varying external heat flux in the computation of OWS temperatures and heat leaks.

A comparison of heat leak data generated by the two models shows good agreement and indicates the successful extension of the MOWS.

(NASA-CR-114031) GENERALIZATION OF THE
SKYLAB ORBITAL WORKSHOP THERMAL MODEL TO
ACCEPT TRANSIENT EXTERNAL ABSORBED HEAT
INPUT DATA (Bellcomm, Inc.) 34 P
CR-114031
FACILITY FO (PAGES)
(NASA CR OR TMX OR AD NUMBER)

(CODE)
(CATEGORY)

N79-12140
00/15 Unclassified
11900



BELLCOMM, INC.

955 L'ENFANT PLAZA NORTH, S.W. WASHINGTON, D.C. 20024

B70 09070

SUBJECT: Generalization of the Skylab
Orbital Workshop Thermal Model
to Accept Transient External
Absorbed Heat Input Data
Case 620

DATE: September 28, 1970
FROM: D. P. Woodard
A. W. Zachar

MEMORANDUM FOR FILE

The MSFC/S&E-ASTN Orbital Workshop (MOWS) thermal model has been generalized to accept transient external heat input data.⁽¹⁾ Preliminary tasks attendant to this generalization have been reported in several previous memoranda⁽²⁾ which we describe briefly: Reference 1 contains a description of the MOWS. The OWS exterior is divided into 96 isothermal surfaces or nodes; the thermal response of the OWS is simulated by applying orbit-average⁽³⁾ absorbed heat rates (BTU/hr) to these surfaces. Reference 2 discusses the computation of incident thermal flux on the OWS surfaces. Reference 3 describes the steps required to convert incident flux to absorbed heat rate and to generate the CINDA compatible transient arrays for input to the BOWS. Table 1 gives the physical constants on which these computations are based, and in addition, defines the sun angle, β .

The new OWS thermal model (BOWS) applies the instantaneous heat absorption rates, $q_{a_i}(t)$, $i = 1, 96$, directly to the external surfaces. This permits the

-
1. We will refer to the MSFC/S&E-ASTN model as the MOWS; the new thermal model, as modified by Bellcomm, will be called the BOWS.
 2. See references attached.
 3. If $q_{a_i}(t)$ is the instantaneous heat absorption rate for external node i , then the orbit-average absorbed heat rate is:

$$\bar{Q}_i = \frac{1}{P} \int_0^P q_{a_i}(t) dt \quad (\text{BTU/hr})$$

where P is the orbit period.

computation of OWS transient temperatures and heat leaks⁽⁴⁾ caused by orbital heat flux variations.⁽⁵⁾ In addition, the BOWS more closely approaches our future need to simulate thermal missions having both time varying internal heat loads and variable orbital heat rates.⁽⁶⁾

The following paragraphs contain comparisons of our orbit-average absorbed heat rates and the rates computed by MSFC/S&E-ASTN. These comparisons show only relatively minor differences. The effects of thermal environmental differences on heat leaks and external surface temperatures are included. In addition, heat leak data generated by both thermal models are compared. The data are in good agreement and indicate the successful transient conversion of the MOWS.

Orbit-Average Environmental Comparisons

Independently computed orbit-average heat flux rates⁽⁷⁾ (BTU/sec ft²) absorbed by the 96 OWS exterior surfaces are compared in Table 2 with flux rates obtained from the MOWS for a Beta angle of 60.5 degrees. Comparison of the two columns shows relatively minor differences except, perhaps, for the solar panels and the thermal impingement curtain, nodes 501 and 502, and nodes 7301 through 7308, respectively.⁽⁸⁾

-
4. Heat leak is taken to be the net heat rate, positive from inside to outside, passing through a given OWS node.
 5. An application of the BOWS transient temperature computation capability is given in Reference 4.
 6. As will be required in "Pick-A-Day" simulations.
 7. Orbit-average heat rates were obtained here by numerically integrating the $q_{a_i}(t)$ which are applied to the BOWS; see footnote (3).
 8. Figure 1 locates the node numbers referenced in Table 2 on the OWS developed surface.

The absorbed heat flux rate differences for the solar arrays are the result of small differences in our incident heat flux rates and absorptance/emittance values. Our values for absorbed heat flux rates are based on α_s/ϵ ratios of .8/.9 and .9/.9 for the front and back sides respectively. Using our orbit-average incident flux rates, we calculate apparent MOWS α_s/ϵ ratios of .86/.9 and .9/.9 for the front and back sides, respectively.

Our lower absorbed thermal impingement curtain flux rates result primarily from a curtain geometry difference. The MOWS rates reflect a truncated cone curtain geometry while the BOWS curtain is modeled as a flat annulus which receives no direct solar illumination. ⁽⁹⁾

Figure 2 compares the total OWS heat leak (BTU/hr) resulting from the orbit average absorbed flux rates contained in Table 2. The time axis begins ($t=0$) with all OWS nodes at 70°F (hence, zero heat leaks) and continues until steady-state equilibrium is reached. In addition to the internal heat sources summarized in Table 3, sufficient heat has been applied to the internal atmosphere to maintain a 70°F gas temperature directly above the common bulkhead. In aggregate, the BOWS orbit-average environment results in an OWS total heat leak some 300 BTU/hr greater than the MOWS value; compare curve 1 and curve 5, Figure 2.

In an attempt to account for this difference, the BOWS orbit-average flux rates were changed to reflect differences in the solar array and thermal impingement curtain flux rates previously discussed. For example, the somewhat higher MOWS solar array flux rates reduce the BOWS heat leak by about 30 BTU/hr; compare curve 1 with curve 2, Figure 2. Further, using the MOWS impingement curtain flux rates, the BOWS leak is reduced by another 160 BTU/hr; compare curve 2 and curve 3. The remaining heat leak difference amounts to somewhat more than 100 BTU/hr, curve 4 vs. curve 5. Table 4 compares these total leaks for the several conditions more precisely and shows, as well, the heat leak components through the several OWS axial divisions. ⁽¹⁰⁾ Note that the major portion of the original total 300 BTU/hr heat leak difference, columns 1 and 2, occurs through the common bulkhead.

-
9. The MOWS truncated cone is a more accurate representation of the curtain geometry.
 10. Each leak component given here is the sum of eight circumferential components.

For completeness, external surface temperatures are given in Table 5 for the several environmental conditions. No obvious discrepancies appear in the data; a higher absorbed heat flux rate yields a higher surface temperature and a lower heat leak.

These data demonstrate that the orbital average heat flux rates used here and at MSFC produce essentially similar data from the BOWS and MOWS programs. Since the orbit-average flux rates are obtained by integration of the time varying rates, these results verify our time varying rates as well.

Transient Environment

We now wish to consider the transient response of the OWS when subjected to transient external heat input and to compare this response with results obtained when orbit average external heat input is used. This will be done for two cases; first, during the first three orbits termed the transient phase and second, during the latter phase after thermal equilibrium has been achieved (after 60 orbits) called the steady state phase.

Figure 3 is concerned with the initial transient response of the OWS and shows the behavior of the total heat leak during the first three orbits. The initial condition is a uniform temperature throughout the OWS of 70°F. Curve 1 gives the OWS total heat leak associated with the BOWS transient external heat input data; curve 2, the total heat leak associated with the BOWS orbit average external environment; curve 3, the heat leak associated with the BOWS orbit average external environment where the MOWS impingement curtain external heat input data have been used; and curve 4, the heat leak associated with the use of the MOWS orbit average external environment. The total heat leak due to the BOWS transient environment (curve 1) is symmetrical about the curve (number 2) which represents the total heat leak due to the BOWS orbit average environment, as might be expected.

Figure 4 gives essentially the same results as mentioned above except that these curves relate to the steady state phase where thermal equilibrium has been achieved. (11)

11. Steady-state has not quite been achieved as indicated by the slightly decreasing peak values bounded by the dashed lines.

Two additional curves are included, however. These are: 1. the total heat leak obtained by averaging, on an orbital basis, the transient heat leak resulting from the application of the BOWS transient external environment (termed BOWS transient average) and, 2. the total heat leak due to the BOWS orbit average heat flux modified through use of the MOWS solar panel heat input data.

Figures 5 through 16 show the component heat leaks due to both BOWS transient and orbit average external environments. In addition, the average of the transient component heat leaks resulting from the application of transient heat input is indicated; designated transient average. These results are summarized in Table 6. The transient average and orbit average curves compare favorably without apparent bias.

Effect of Non-Linearities and Transient Thermal Environment

During a portion of this study, the authors were concerned with the possible effect on OWS heat leaks of both non linear⁽¹²⁾ radiation and conduction heat transfer paths and the use of orbit-average environmental heat inputs. This subject is developed in detail in the Appendix. In view of the close agreement between the transient-average and orbit-average derived heat leak components, we conclude that the magnitude of these non-linear effects on the OWS thermal behavior is small.

Acknowledgements

The authors wish to acknowledge the contributions of Mr. J. W. Powers for incident heat data and of Mrs. B. W. Lab for her programming assistance.

D. P. Woodard

A. W. Sachar

1022-DPW-rl
AWZ

Attachments

References

Tables 1-6

Figures 1-16

Appendix

Table A-1

BELLCOMM, INC.

REFERENCES

1. *Skylab Orbital Workshop Thermal Model, Memorandum for File, Case 620, June 30, 1970, D. P. Woodard, A. W. Zachar*
2. *Incident Thermal Fluxes on Skylab Surfaces for the "Pick-A-Day" Mission, Memorandum for File, Case 620, July 2, 1970, J. W. Powers.*
3. *Generation of OWS External Shell Transient Absorbed Heat Arrays, Memorandum for File, Case 620, April 10, 1970, A. W. Zachar*
4. *Skylab LOX Tank Vent Lines and Nozzle Temperatures, Memorandum for File, Case 620, September 21, 1970, D. P. Woodard.*

TABLE 1

FLUX PHYSICAL DATA

SOLAR CONSTANT = 429 BTU/FT² HR

EARTH ALBEDO = .30

ORBIT DATA

PERIGEE = 271 MILES

ECCENTRICITY = 0

EARTH RADIUS = 3960 MILES

POSITIVE β DEFINED

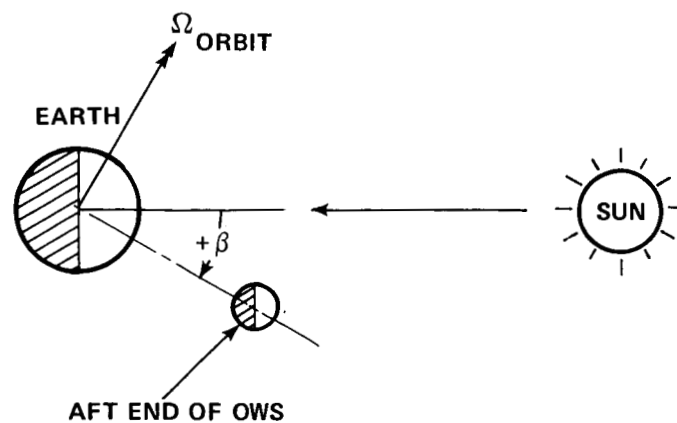


TABLE 2
ORBIT AVERAGE HEAT FLUX COMPARISONS

	NODES	MOWS (BTU/SEC FT ²)	BOWS (BTU/SEC FT ²)
SOLAR PANELS	501 502	.09129 .09129	.08543 .08543
AIRLOCK SHROUD	1111 1112 1113 1114	.06070 .05849 .00647 .01031	.06469 .06375 .00605 .00944
INSTRUMENT UNIT	1211 1212 1213 1214 1215 1216 1217 1218	.03969 .08171 .08012 .03685 .00606 .00687 .00950 .01111	.03936 .08149 .08101 .03755 .00597 .00654 .00840 .00982
UPPER FORWARD SKIRT	1311 1312 1313 1314 1315 1316 1317 1318	.03969 .08171 .08012 .03685 .00606 .00687 .00940 .01111	.03936 .08149 .08101 .03755 .00597 .00654 .00840 .00982
LOWER FORWARD SKIRT	1411 1412 1413 1414 1415 1416 1417 1418	.03969 .08171 .08012 .03685 .00606 .00687 .00940 .01111	.03936 .08149 .08101 .03755 .00597 .00654 .00840 .00982
FORWARD METEOROID SHIELD EXTENSION	541 542 543 544 545 546 547 548	.03969 .08171 .08012 .03685 .00606 .00687 .00940 .01111	.03936 .08149 .08101 .03755 .00597 .00654 .00840 .00982
METEOROID SHIELD TOP	510 511 512 513 514 515 516 517 518 519	.03969 .03969 .08171 .08012 .03685 .00606 .00687 .00950 .01111	.03935 .03936 .08149 .08101 .03755 .00597
METEOROID SHIELD BOTTOM	520 521 522 523 524 525 526 527 528 529	.03969 .03969 .08171 .08012 .03685 .00606 .00687 .00950 .01111	.03935 .03936 .08149 .08101 .03755 .00597
AFT METEOROID SHIELD EXTENSION	531 532 533 534 535 536 537 538	.03969 .08171 .08012 .03685 .00606 .00687 .00950 .01111	.03936 .08149 .08101 .03755 .00597 .00654 .00840 .00982
LOWER AFT SKIRT 1	7401 7402 7403 7404 7405 7406 7407 7408	.03969 .08171 .08012 .03685 .00606 .00687 .00950 .01111	.03936 .08149 .08101 .03755 .00597 .00654 .00840 .00982
LOWER AFT SKIRT 2	7201 7202 7203 7204 7205 7206 7207 7208	.01916 .03524 .03534 .01852 .00572 .00578 .00728 .00820	.01909 .03576 .03593 .01888 .00575 .00578 .00687 .00776
IMPINGEMENT CURTAIN	7301 7302 7303 7304 7305 7306 7307 7308	.01769 .02961 .02901 .01657 .00775 .00823 .00876 .00913	.00795 .00795 .00795 .00795 .00795 .00795 .00795 .00795
THRUST CONE	8101 8102 8103 8104 8105 8106 8107 8108	.02756 .05356 .05297 .02510 .00588 .00650 .00801 .00893	.02621 .05196 .05162 .02497 .00581 .00617 .00722 .00801

TABLE 3
INTERNAL HEAT SOURCES – BTU/HR

	CONVECTION	RADIATION	TOTAL
ABOVE CREW QUARTERS	132.5	330.5	463.0
CREW QUARTERS WORK COMPARTMENT	420.0	623.0	1043.0
CREW QUARTERS SLEEP COMPARTMENT 1	45.0	67.0	112.0
CREW QUARTERS WASTE COMPARTMENT	45.0	67.0	112.0
CREW QUARTERS FOOD COMPARTMENT	54.7	96.3	151.0
CREW QUARTERS SLEEP COMPARTMENT 2	45.0	67.0	112.0
BELOW CREW QUARTERS	19.5	58.5	78.0

TABLE 4
COMPARISON OF ORBIT AVERAGE HEAT LEAK COMPONENTS – BTU/HR

COMPONENT	MOWS ORBIT AVERAGE	BOWS ORBIT AVERAGE	BOWS ORBIT AVERAGE W/MOWS CURTAIN	BOWS ORBIT AVERAGE W/MOWS S/A	BOWS ORBIT AVERAGE W/MOWS S/A AND CURTAIN
Q _{TOTAL}	1489.8	1776.0	1621.6	1746.2	1591.8
UPPER FWD. DOME	184.3	181.3	183.8	179.6	182.1
LOWER FWD. DOME	70.1	73.3	75.6	70.7	73.0
FWD. JOINT	47.2	51.0	53.7	48.1	50.8
UPPER ABOVE CQ SIDEWALL	- 49.1	-39.6	-35.3	-45.8	-41.4
LOWER ABOVE CQ SIDEWALL	-101.3	-92.3	-88.9	-98.1	-94.7
CREW QUARTERS (CQ) SIDEWALL	- 72.9	-62.2	-57.6	-68.0	-63.4
BELOW CQ SIDEWALL	- 42.3	-41.3	-31.6	-45.5	-35.9
AFT JOINT	90.3	94.7	94.5	93.7	93.6
AFT FUEL DOME	278.9	297.4	286.1	295.8	284.6
COMMON BULKHEAD (CB)	1043.8	1268.5	1099.1	1270.6	1101.2
CB TO LH2 AFT DOME	19.1	19.2	19.6	19.1	19.5
CB TO LOX DOME	21.5	26.1	22.4	26.1	22.5
FOOTNOTE	(1)	(2)	(3)	(4)	(5)
RUN I.D.		060970	061070	060470	060570

- (1) MOWS ORBIT AVERAGE ABSORBED EXTERNAL HEAT LOADS
- (2) BOWS ORBIT AVERAGE ABSORBED EXTERNAL HEAT LOADS
- (3) BOWS ORBIT AVERAGE ABSORBED EXTERNAL HEAT LOADS BUT WITH MOWS ORBIT AVERAGE ABSORBED IMPINGEMENT CURTAIN LOAD
- (4) BOWS ORBIT AVERAGE ABSORBED EXTERNAL HEAT LOADS BUT WITH MOWS ORBIT AVERAGE ABSORBED SOLAR ARRAY LOADS
- (5) BOWS ORBIT AVERAGE ABSORBED EXTERNAL HEAT LOADS BUT WITH MOWS ORBIT AVERAGE ABSORBED SOLAR ARRAY AND IMPINGEMENT CURTAIN HEAT LOADS

TABLE 5
ORBIT AVERAGE EXTF VAL TEMPERATURE COMPARISONS

	NODES	TEMP. MOWS (°F)	TEMP. BOWS (°F)	TEMPERATURE BOWS W/MOWS IMPIGNEMENT CURTAIN (°F)	TEMPERATURE BOWS W/MOWS SOLAR ARRAY (°F)	TEMPERATURE BOWS W/MOWS SOLAR ARRAY & CURTAIN (°F)
SOLAR PANELS	501	89.5	80.6	80.6	89.4	89.4
	502	88.4	79.7	79.7	88.4	88.4
AIRLOCK SHROUD	1111	114.5	122.2	122.2	122.2	122.2
	1112	109.4	119.7	119.7	119.8	119.8
	1113	- 48.7	- 49.4	- 49.4	- 49.3	- 49.3
	1114	- 32.5	- 35.4	- 35.4	- 35.3	- 35.3
INSTRUMENT UNIT	1211	90.9	90.3	90.3	90.7	90.7
	1212	161.2	161.3	161.3	161.3	161.3
	1213	159.3	161.3	161.3	161.3	161.3
	1214	81.0	83.1	83.2	83.5	83.5
	1215	- 36.4	- 36.8	- 36.8	- 35.8	- 35.8
	1216	- 55.7	- 57.1	- 57.1	- 56.8	- 56.8
	1217	- 41.5	- 47.0	- 47.0	- 46.8	- 46.8
	1218	- 14.6	- 20.4	- 20.4	- 19.7	- 19.7
UPPER FORWARD SKIRT	1311	97.5	96.5	96.5	97.1	97.1
	1312	168.3	168.4	168.4	168.4	168.5
	1313	164.6	166.5	166.5	166.6	166.6
	1314	85.0	87.0	87.1	87.5	87.5
	1315	- 32.2	- 33.2	- 33.2	- 31.8	- 31.8
	1316	- 64.0	- 66.5	- 66.5	- 66.1	- 66.1
	1317	- 50.0	- 57.0	- 57.0	- 56.8	- 56.8
	1318	- 10.6	- 17.2	- 17.2	- 16.3	- 16.3
LOWER FORWARD SKIRT	1411	94.7	93.7	93.7	94.2	94.3
	1412	170.2	170.3	170.3	170.3	170.4
	1413	166.3	168.2	168.2	168.3	168.3
	1414	86.7	88.6	88.6	89.2	89.2
	1415	- 19.7	- 21.4	- 21.4	- 19.5	- 19.5
	1416	- 58.6	- 61.0	- 61.0	- 60.7	- 60.6
	1417	- 44.9	- 51.4	- 51.4	- 51.2	- 51.2
	1418	- 7.7	- 14.4	- 14.3	- 13.3	- 13.3
FORWARD METEOROID SHIELD EXTENSION	541	110.5	108.4	108.4	109.4	109.4
	542	199.2	198.7	198.7	198.7	198.8
	543	194.8	196.5	196.5	196.6	196.6
	544	99.2	100.6	100.6	101.5	101.5
	545	- 39.3	- 43.1	- 43.1	- 40.0	- 40.0
	546	- 85.8	- 89.9	- 89.9	- 89.5	- 89.4
	547	- 64.4	- 74.9	- 74.9	- 74.8	- 74.8
	548	- 17.6	- 28.4	- 28.4	- 26.4	- 26.4
METEOROID SHIELD TOP	510	110.2	108.1	108.1	109.1	109.1
	511	105.1	103.3	103.3	104.0	104.0
	512	199.5	199.0	199.0	199.1	199.1
	513	195.0	196.7	196.8	196.8	196.8
	514	101.6	102.9	102.9	103.9	103.9
	515	- 29.3	- 33.5	- 33.5	- 30.0	- 30.0
	516	- 75.2	- 77.7	- 77.7	- 76.2	- 76.2
	517	- 85.3	- 89.5	- 89.5	- 89.0	- 89.0
	518	- 64.3	- 75.0	- 75.0	- 74.8	- 74.8
	519	- 13.3	- 24.2	- 24.2	- 22.0	- 22.0
METEOROID SHIELD BOTTOM	520	104.3	102.5	102.5	103.2	103.2
	521	100.3	98.7	98.7	99.2	99.2
	522	199.0	198.5	198.5	198.6	198.6
	523	194.8	196.6	196.6	196.6	196.6
	524	97.3	98.8	98.8	99.6	99.6
	525	- 47.2	- 50.8	- 50.7	- 50.0	- 47.9
	526	- 84.6	- 88.7	- 88.6	- 85.6	- 85.6
	527	- 87.4	- 91.6	- 91.5	- 91.2	- 91.1
	528	- 64.7	- 75.4	- 75.4	- 75.3	- 75.2
	529	- 21.1	- 32.0	- 31.9	- 30.2	- 30.1
AFT METEOROID SHIELD EXTENSION	531	94.5	93.1	93.2	93.3	93.4
	532	198.0	197.4	197.5	197.5	197.5
	533	194.3	196.0	196.1	196.1	196.1
	534	89.9	91.7	91.8	92.2	92.3
	535	- 84.1	- 86.3	- 86.1	- 85.2	- 85.1
	536	- 90.6	- 94.7	- 94.6	- 94.5	- 94.3
	537	- 65.5	- 76.1	- 76.0	- 76.0	- 75.9
	538	- 35.5	- 46.6	- 46.5	- 45.6	- 45.4
LOWER AFT SKIRT 1	7401	74.0	71.1	72.8	71.3	73.0
	7402	169.4	167.6	169.1	167.7	169.2
	7403	166.1	168.4	167.9	166.4	167.9
	7404	69.3	69.4	71.0	69.8	71.4
	7405	- 52.9	- 54.6	- 53.8	- 54.1	- 53.3
	7406	- 71.5	- 74.4	- 73.5	- 74.2	- 73.4
	7407	- 44.7	- 51.3	- 50.4	- 51.2	- 50.3
	7408	- 24.7	- 32.2	- 31.1	- 31.6	- 30.5
LOWER AFT SKIRT 2	7201	18.6	11.7	17.8	11.9	18.0
	7202	79.3	72.7	80.5	72.8	80.6
	7203	78.6	72.6	80.2	72.7	80.3
	7204	17.2	12.8	16.3	13.2	18.7
	7205	- 71.6	- 73.3	- 72.1	- 72.9	- 71.6
	*7206	- 121.7	- 124.3	- 122.9	- 124.1	- 122.7
	7207	- 71.7	- 77.2	- 75.6	- 77.1	- 75.5
	7208	- 48.2	- 54.7	- 52.2	- 54.1	- 51.8
IMPINGEMENT CURTAIN	7301	8.5	- 42.8	7.9	- 42.7	7.9
	7302	66.5	- 25.0	66.2	- 24.9	66.2
	7303	64.2	- 25.1	64.1	- 25.1	64.1
	7304	2.5	- 43.2	2.4	- 43.1	2.5
	7305	- 68.1	- 68.1	- 68.5	- 68.1	- 68.5
	7306	- 71.2	- 74.8	- 71.9	- 74.7	- 71.9
	7307	- 63.9	- 71.8	- 65.4	- 71.6	- 65.3
	7308	- 54.1	- 64.1	- 55.5	- 64.0	- 55.4
THRUST CONE	8101	55.1	44.0	51.0	44.0	51.1
	8102	107.9	96.1	104.2	96.1	104.2
	8103	106.4	95.3	103.1	95.3	103.2
	8104	48.9	40.8	47.4	40.9	47.5
	8105	- 18.4	- 23.2	- 70.1	- 23.1	- 20.1
	8106	- 10.2	- 16.2	- 12.8	- 16.2	- 12.7
	8107	- 28.7	- 36.9	- 33.4	- 36.8	- 33.1
	8108	- 8.4	- 17.0	- 13.0	- 16.9	- 13.0
RUN I.D.			060970	061070	060470 2C	060570 2D

*THIS TEMPERATURE IS INCORRECT DUE TO A PUNCH ERROR IN THE MOWS MODEL.

TABLE 6
COMPARISON OF BOWS ORBIT AVERAGE AND STEADY STATE
AVERAGE HEAT LEAK COMPONENTS – BTU/HR

COMPONENT	BOWS ORBIT AVERAGE	BOWS STEADY STATE AVERAGE
Q _{TOTAL}	1776.0	1797.6
UPPER FWD. DOME	181.3	190.7
LOWER FWD. DOME	73.3	79.2
FWD. JOINT	51.0	57.8
UPPER ABOVE CQ SIDEWALL	-39.6	-35.6
LOWER ABOVE CQ SIDEWALL	-92.3	-92.1
CREW QUARTERS (CQ) SIDEWALL	-62.2	-61.4
BELOW CQ SIDEWALL	-41.3	-42.4
AFT JOINT	94.7	93.1
AFT FUEL DOME	297.4	292.2
COMMON BULKHEAD (CB)	1268.5	1271.3
CB TO LH2 AFT DOME	19.2	18.6
CB TO LOX DOME	26.1	26.0
FOOTNOTE	(1)	(2)
RUN I.D.	060970	060970

- (1) BOWS ORBIT AVERAGE ABSORBED EXTERNAL HEAT LOADS
- (2) BOWS TRANSIENT ABSORBED HEAT LOADS - AVERAGE OVER AN ORBIT AFTER STEADY STATE

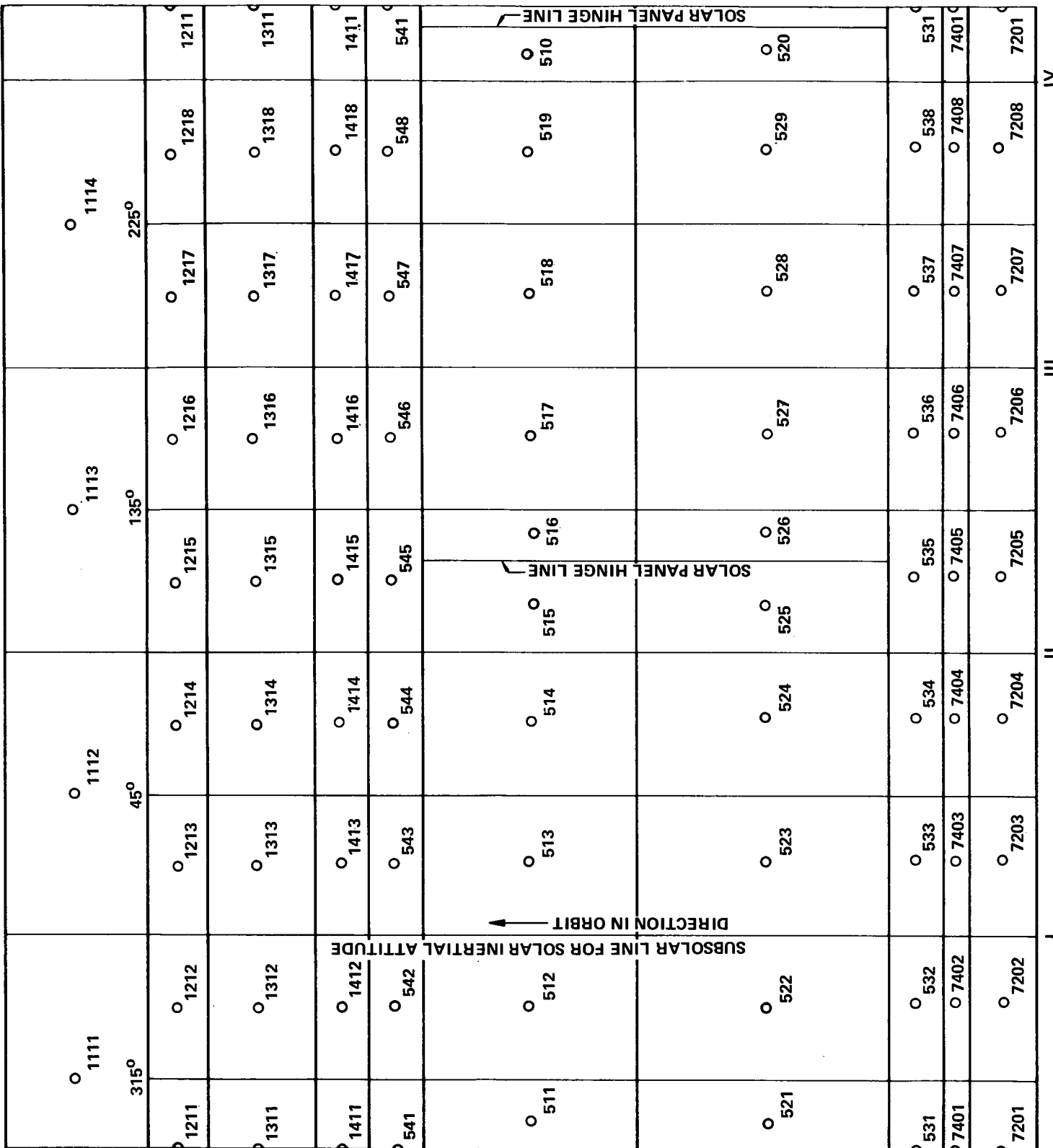


FIGURE 1 - CIRCUMFERNENTIAL LOCATION OF EXTERIOR THERMAL NODES

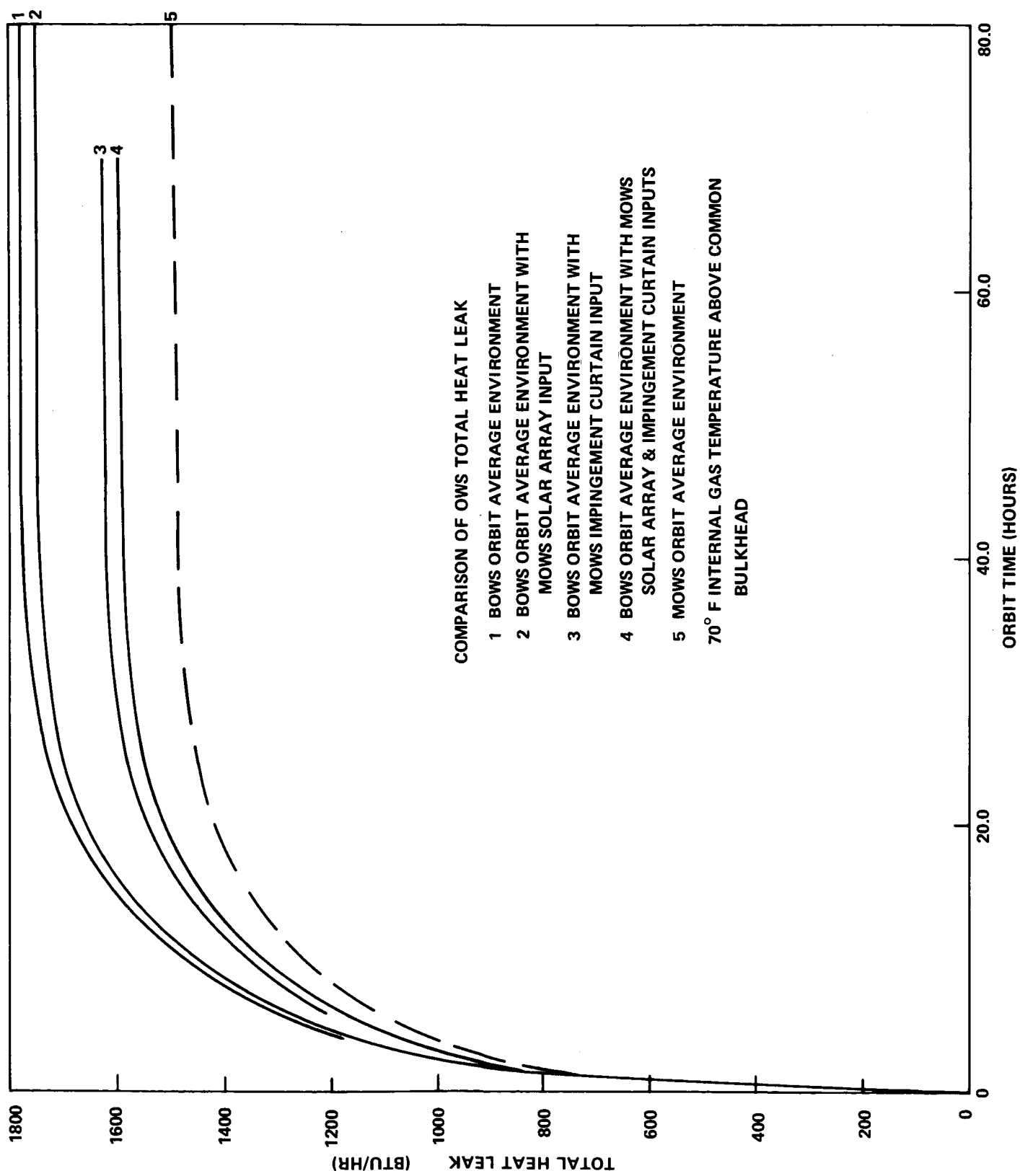


FIGURE 2 - OWS TOTAL HEAT LEAK, $\beta = 60.5^{\circ}$

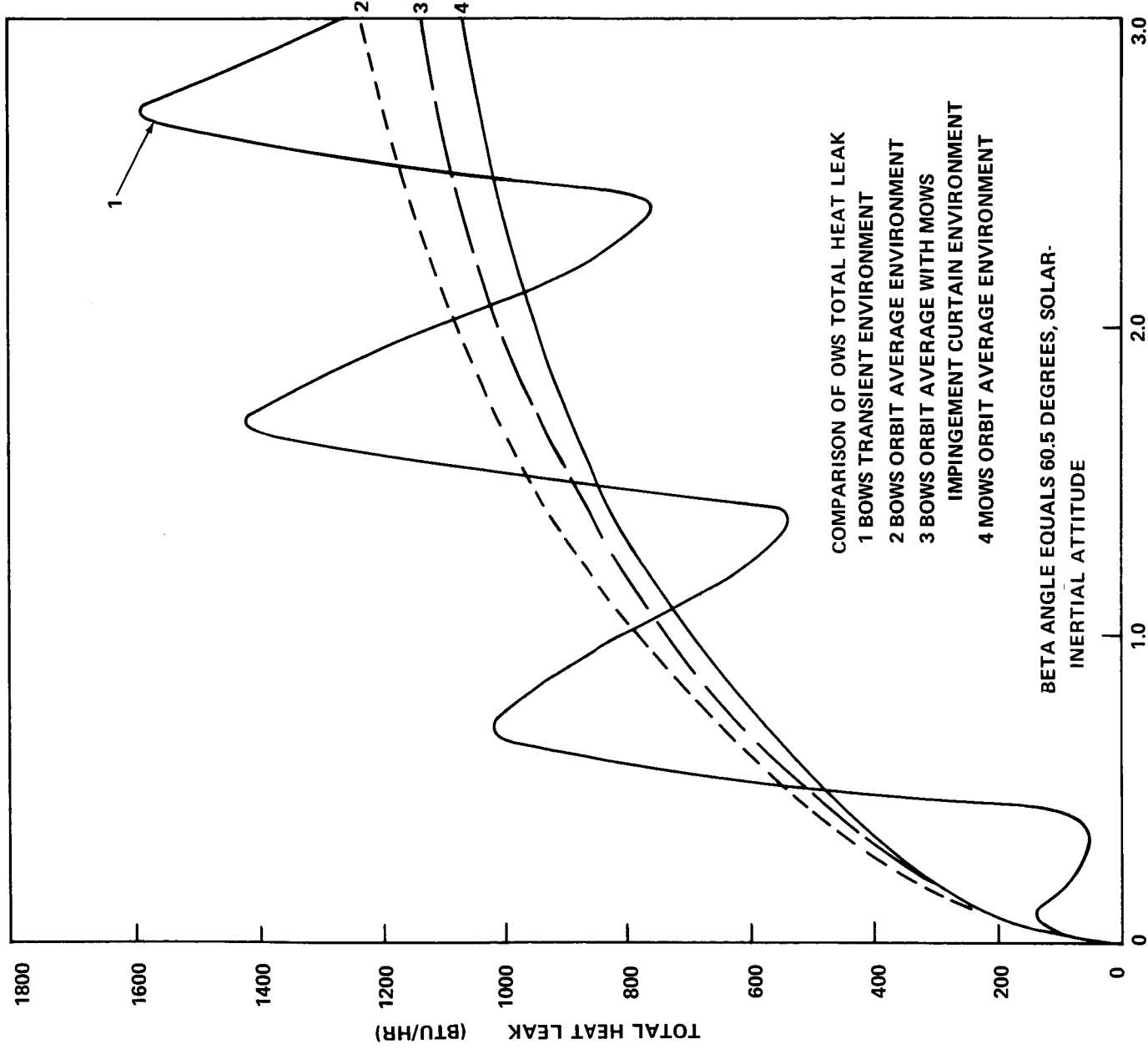


FIGURE 3 - TRANSIENT AND ORBIT AVERAGE OWS TOTAL HEAT LEAK

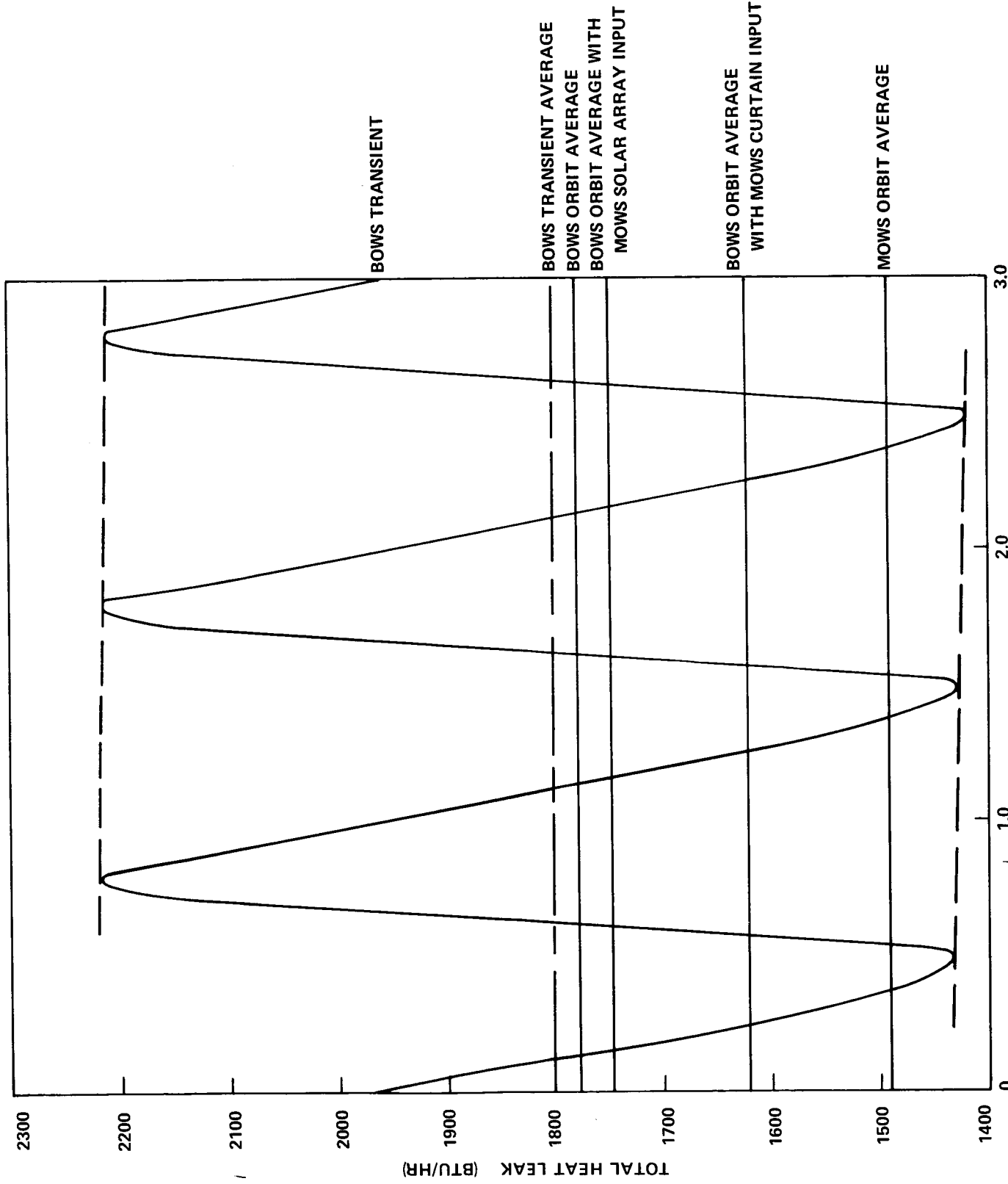


FIGURE 4 - TOTAL OWS TRANSIENT HEAT LEAK, STEADY STATE

$$\beta = 60.5^\circ$$

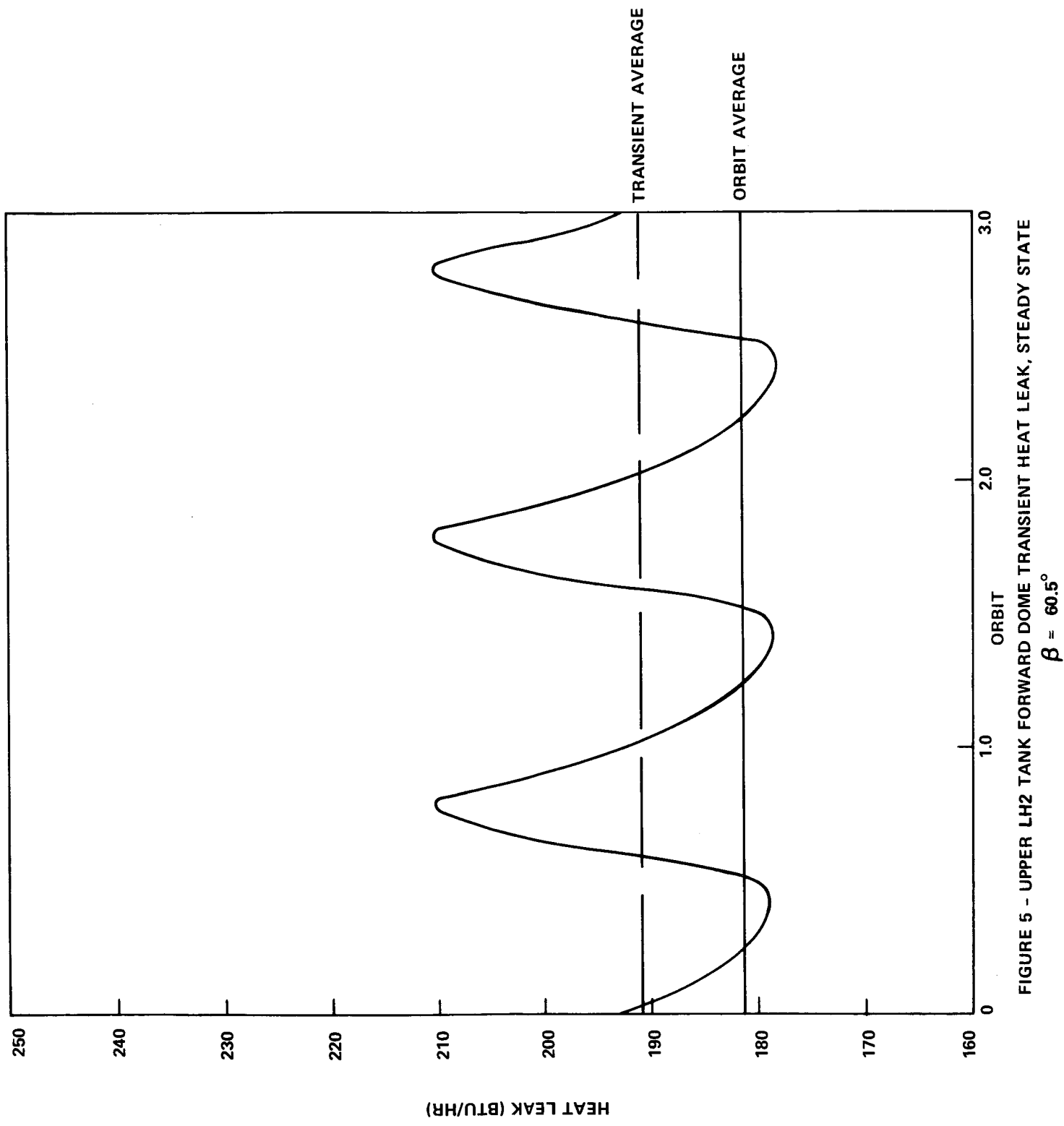


FIGURE 5 - UPPER LH₂ TANK FORWARD DOME TRANSIENT HEAT LEAK, STEADY STATE
 $\beta = 60.5^\circ$

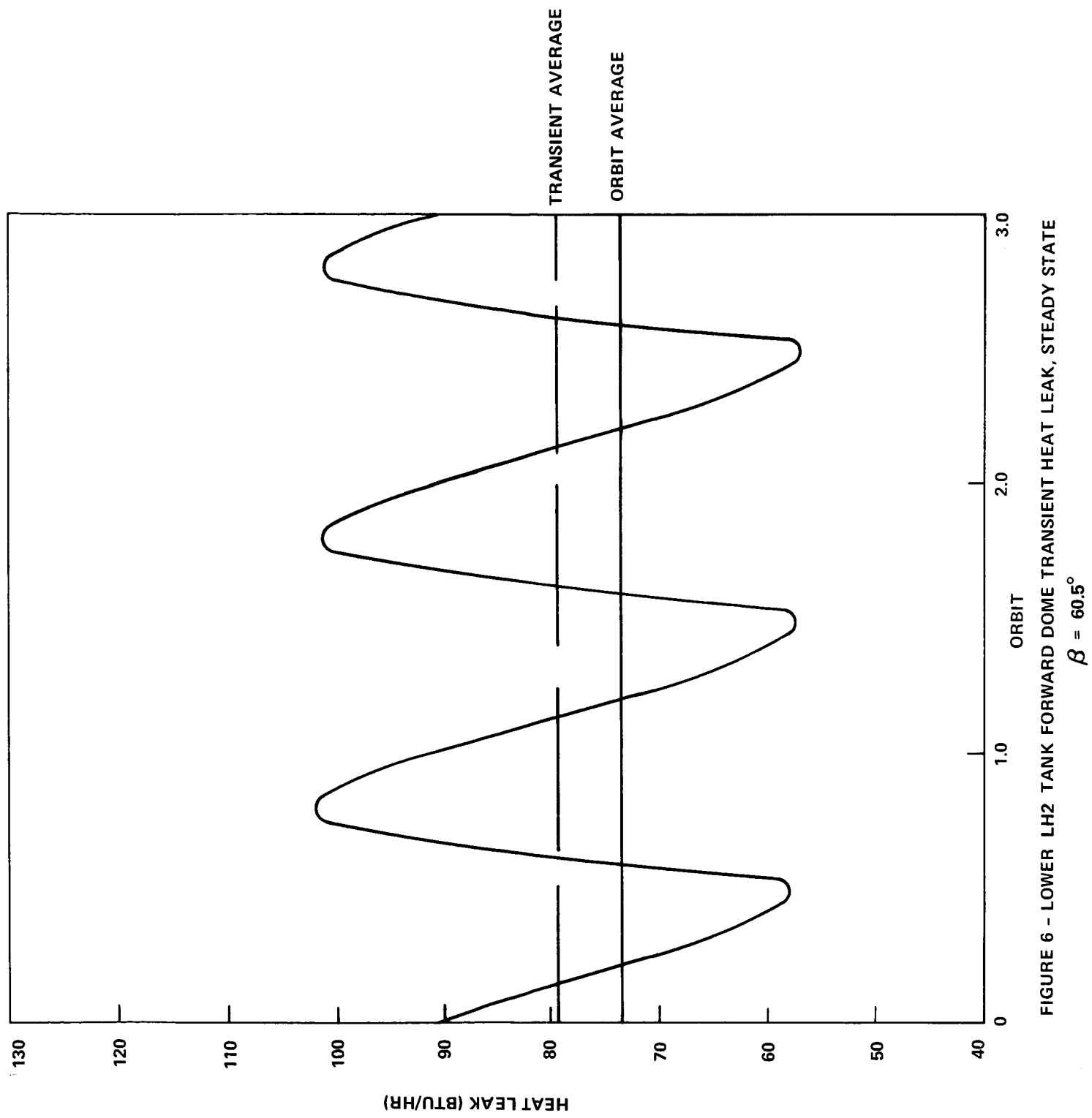


FIGURE 6 - LOWER LH₂ TANK FORWARD DOME TRANSIENT HEAT LEAK, STEADY STATE
 $\beta = 60.5^\circ$

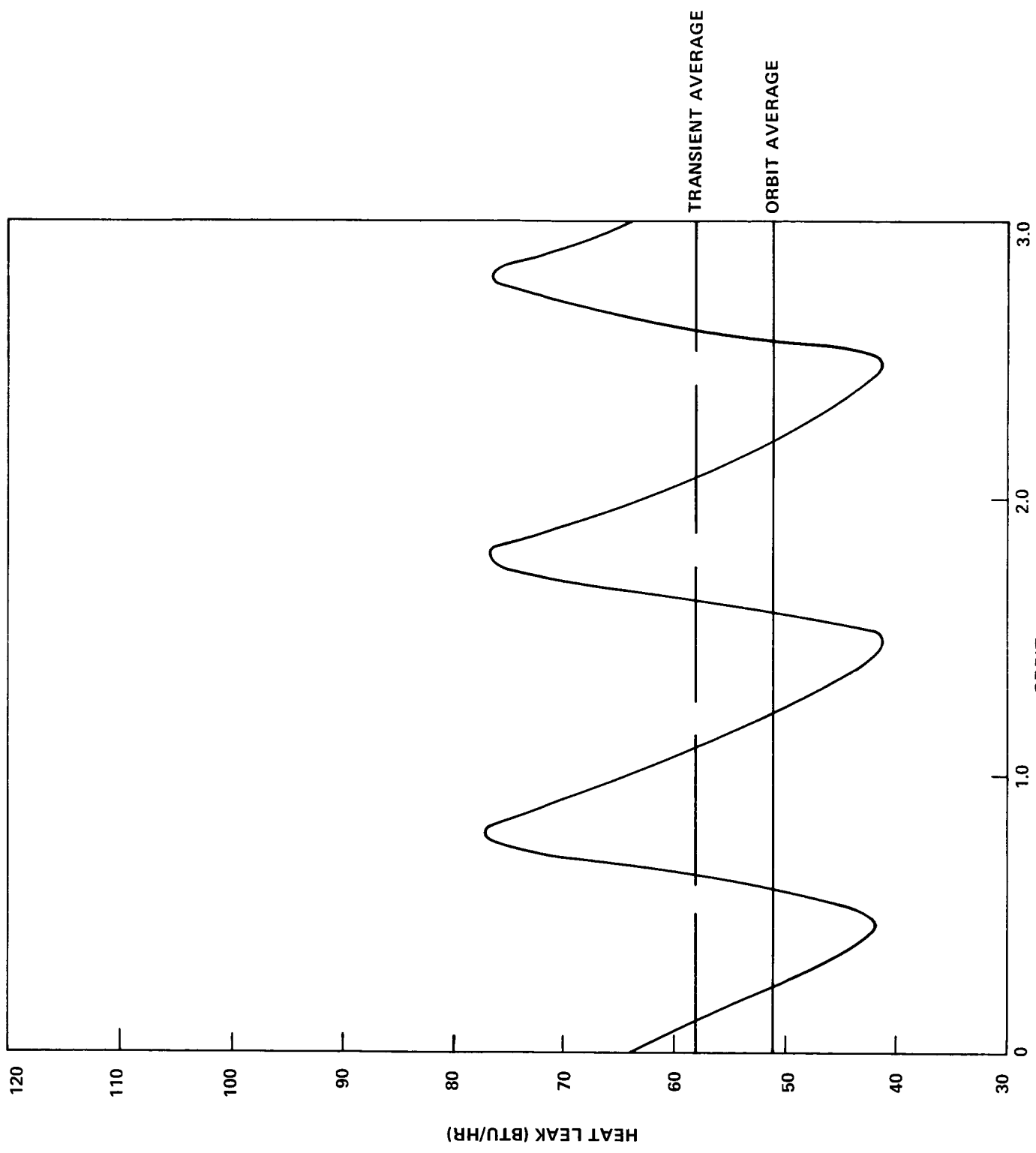


FIGURE 7 - FORWARD JOINT TRANSIENT HEAT LEAK, STEADY STATE
 $\beta = 60.5^\circ$

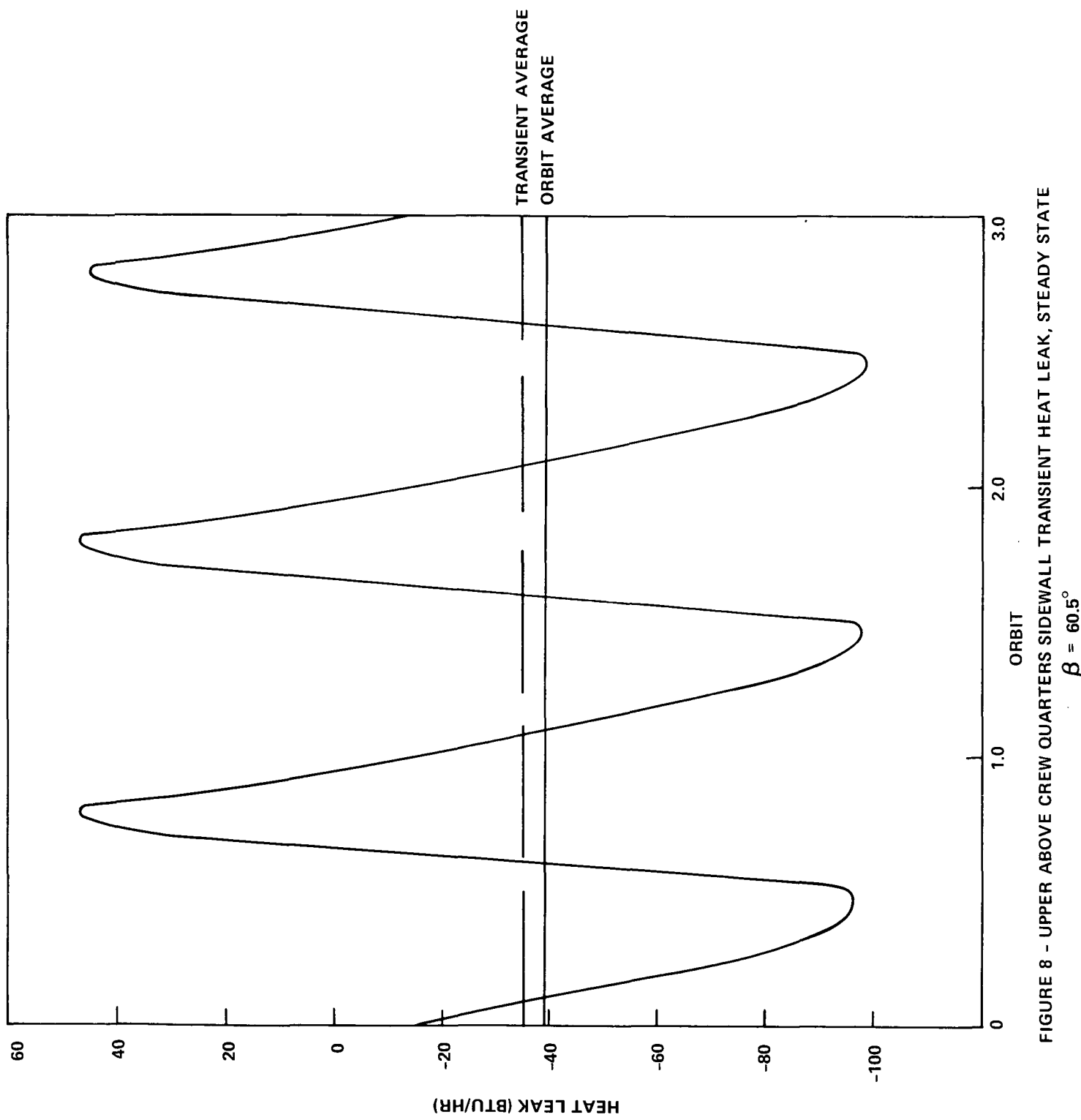


FIGURE 8 - UPPER ABOVE CREW QUARTERS SIDEWALL TRANSIENT HEAT LEAK, STEADY STATE
 $\beta = 60.5^\circ$

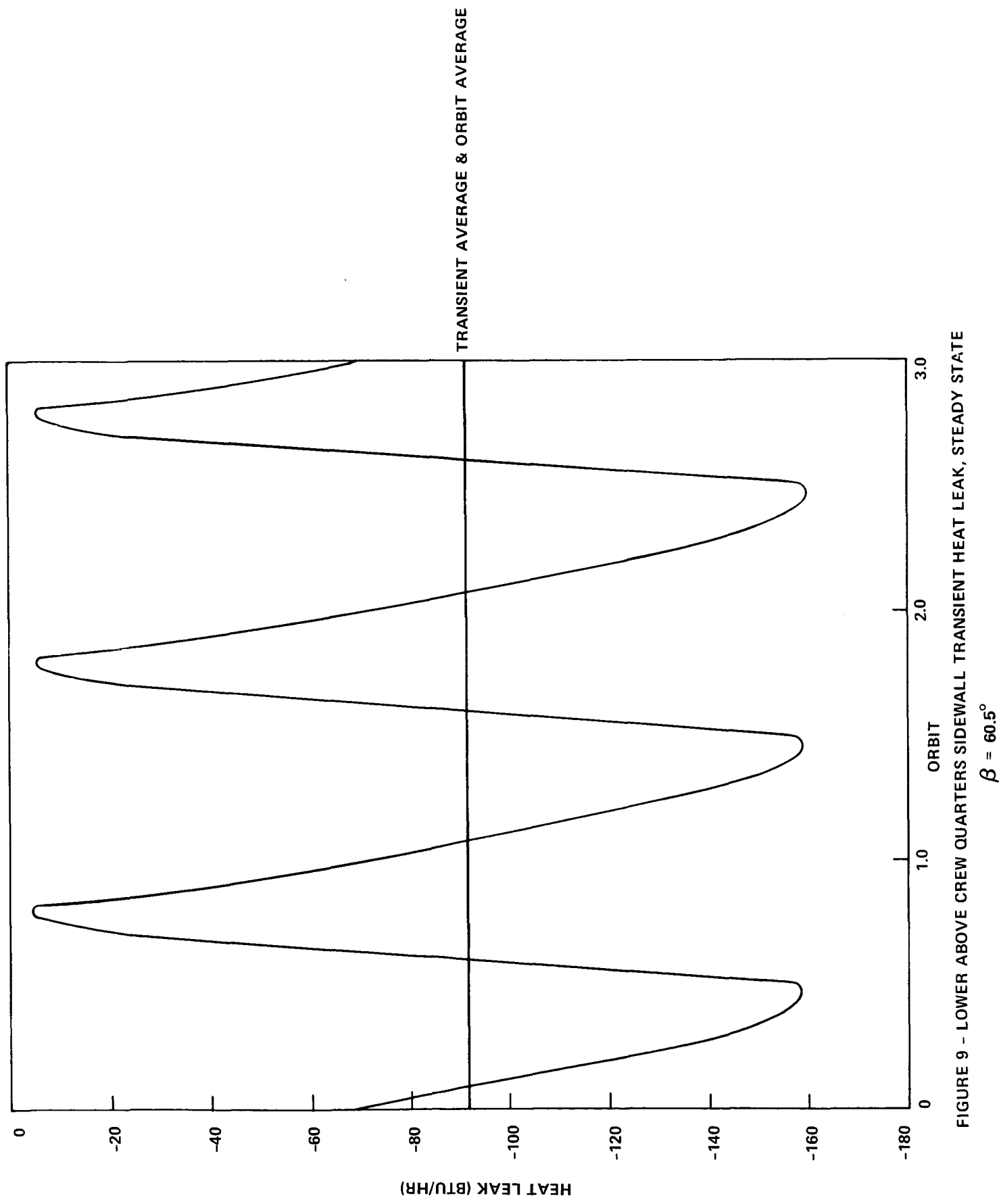


FIGURE 9 - LOWER ABOVE CREW QUARTERS SIDEWALL TRANSIENT HEAT LEAK, STEADY STATE
 $\beta = 60.5^\circ$

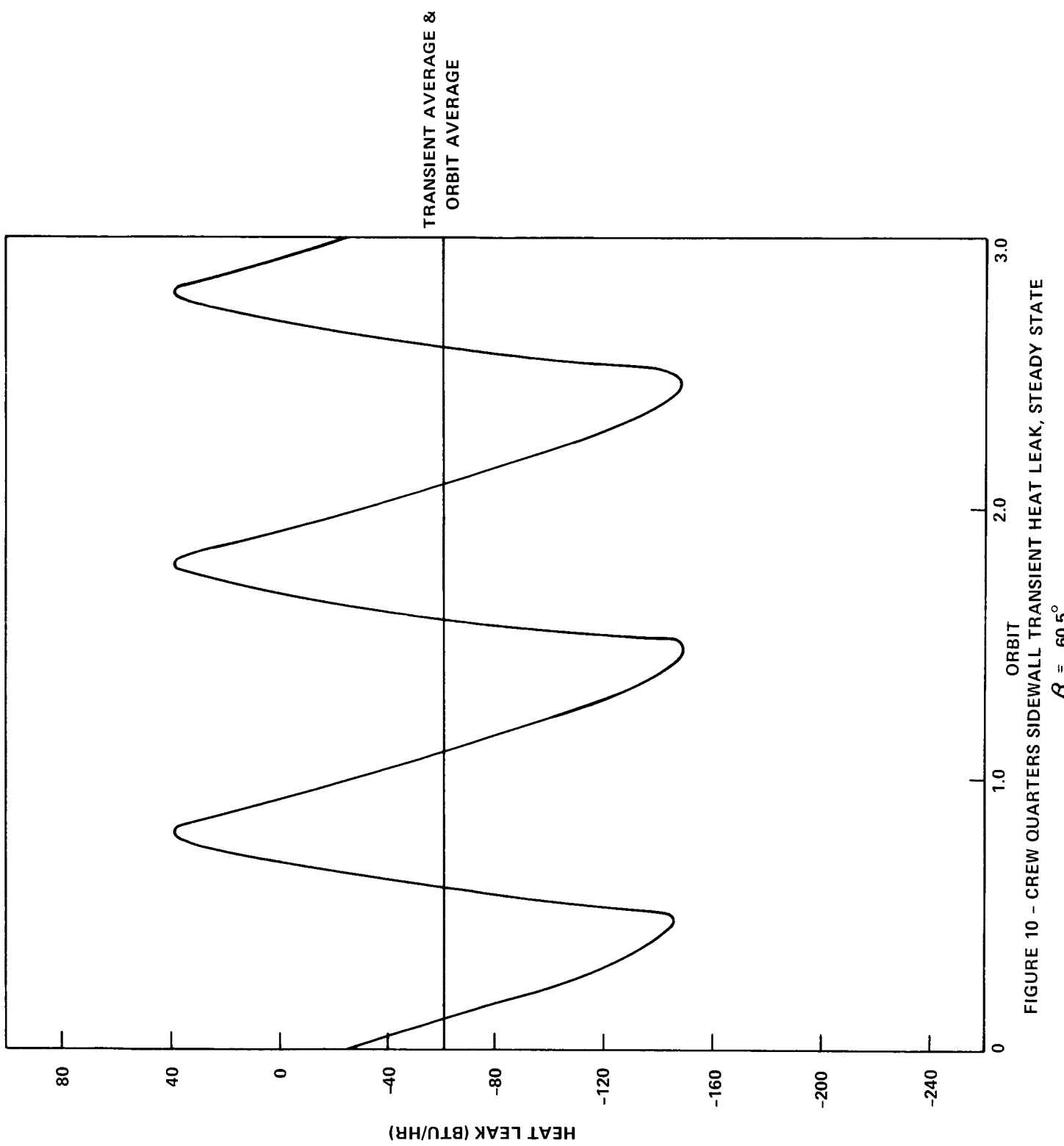
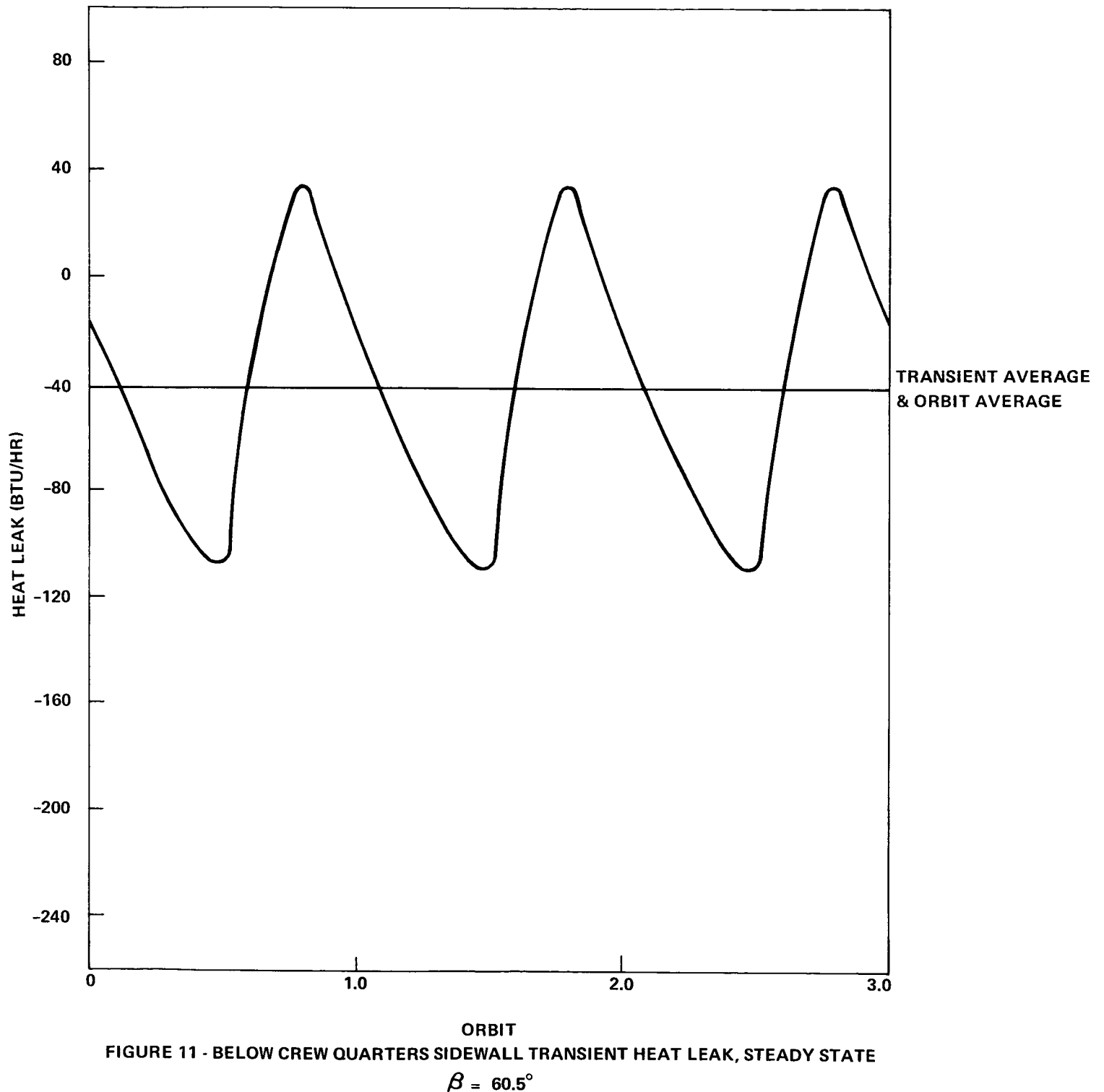


FIGURE 10 - CREW QUARTERS SIDEWALL TRANSIENT HEAT LEAK, STEADY STATE
 $\beta = 60.5^\circ$



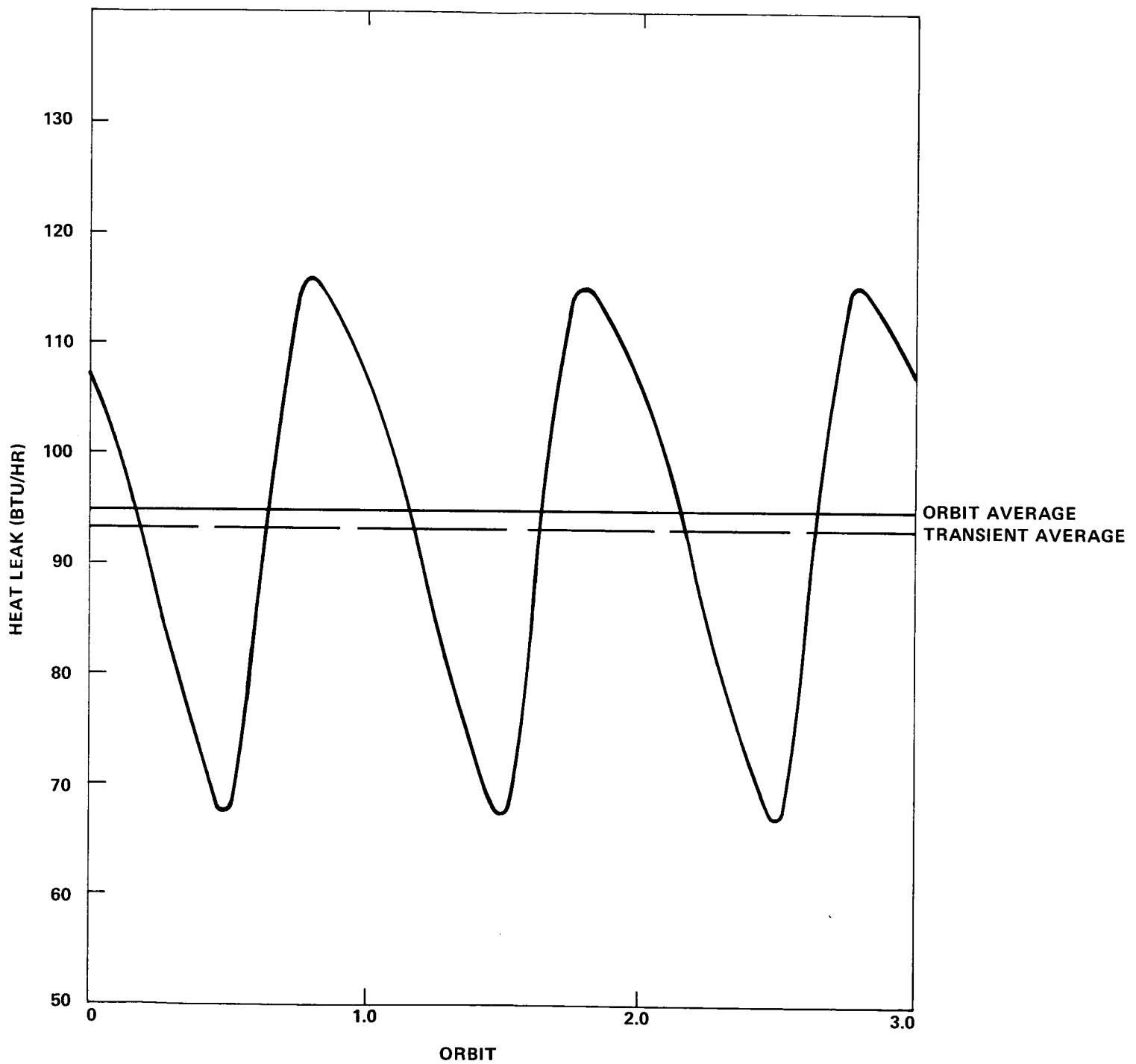


FIGURE 12 - AFT JOINT TRANSIENT HEAT LEAK, STEADY STATE

$$\beta = 60.5^\circ$$

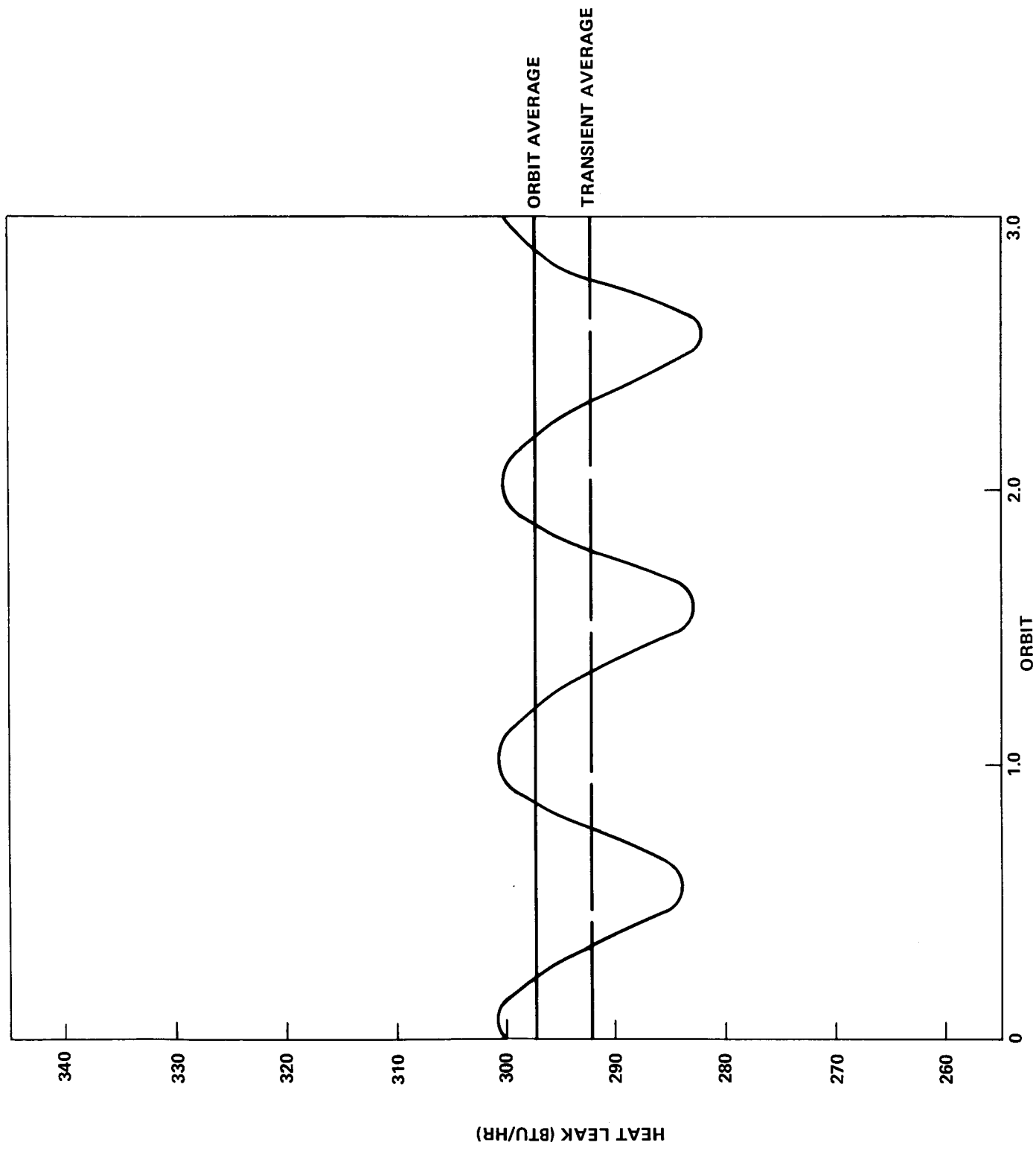


FIGURE 13 - AFT LH₂ TANK DOME TRANSIENT HEAT LEAK, STEADY STATE

$$\beta = 60.5^\circ$$

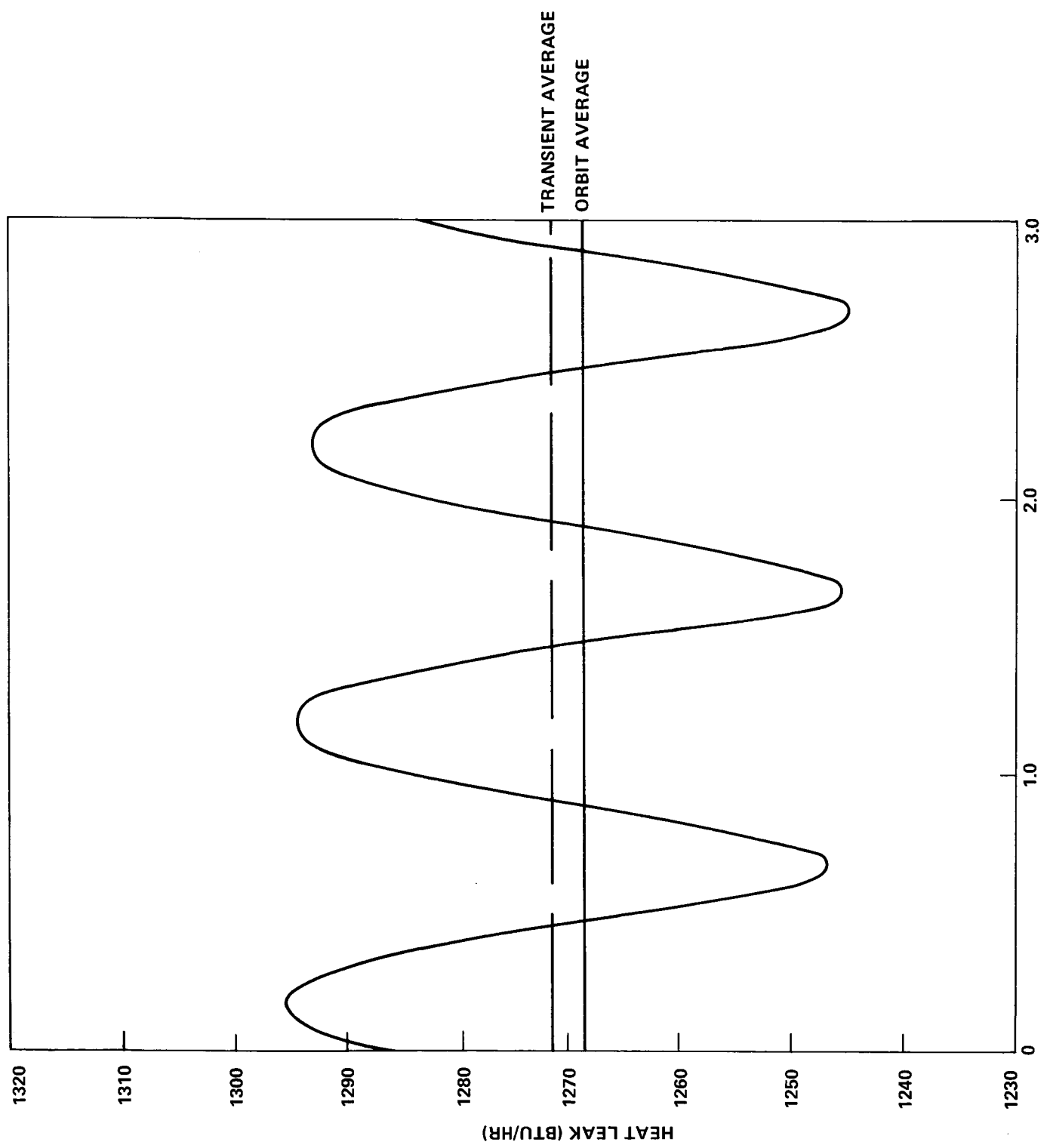


FIGURE 14 - COMMON BULKHEAD TRANSIENT HEAT LEAK, STEADY STATE $\beta = 60.5^\circ$

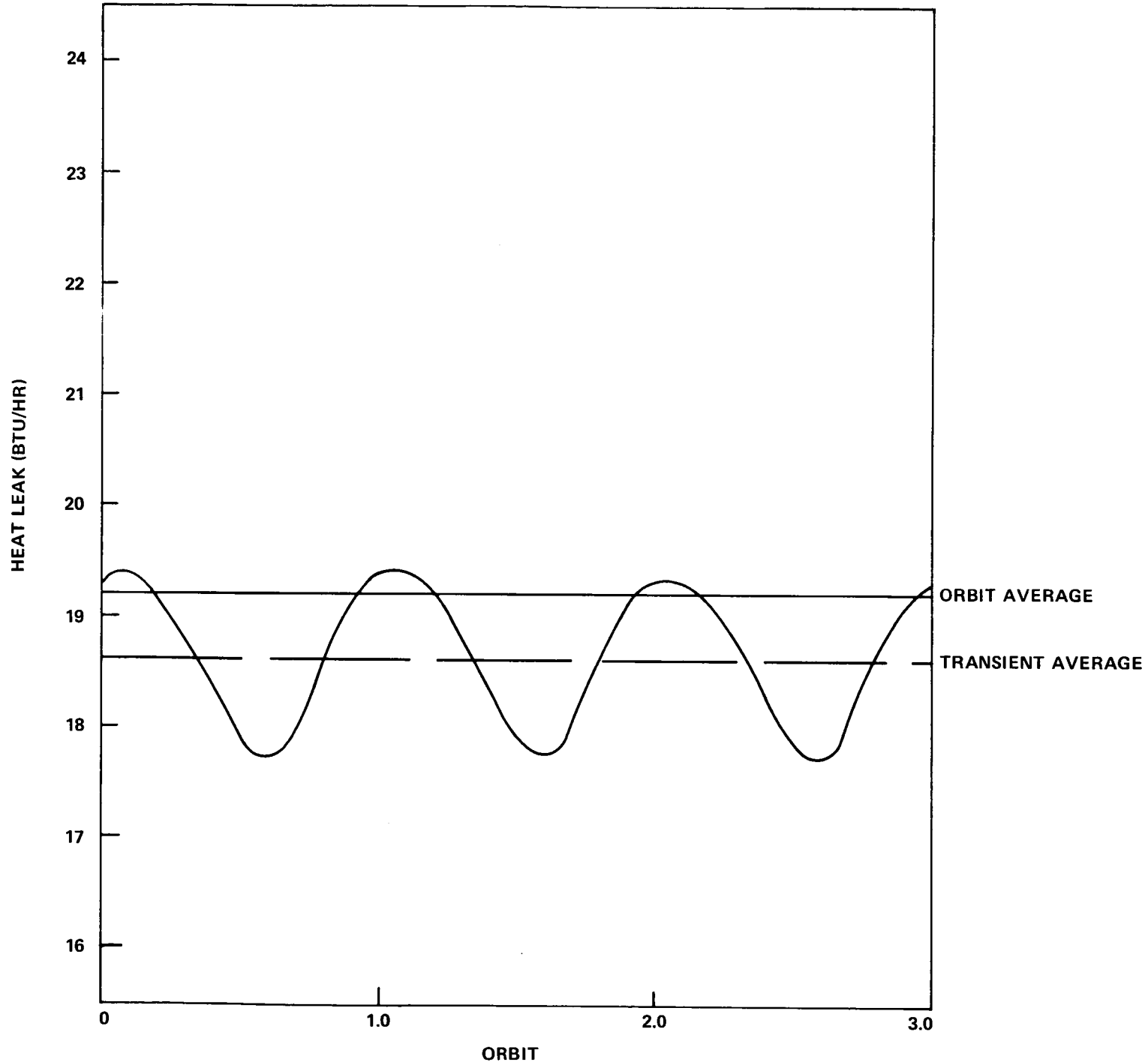


FIGURE 15 - COMMON BULKHEAD TO AFT LH₂ TANK DOME TRANSIENT HEAT LEAK, STEADY STATE

$$\beta = 60.5^\circ$$

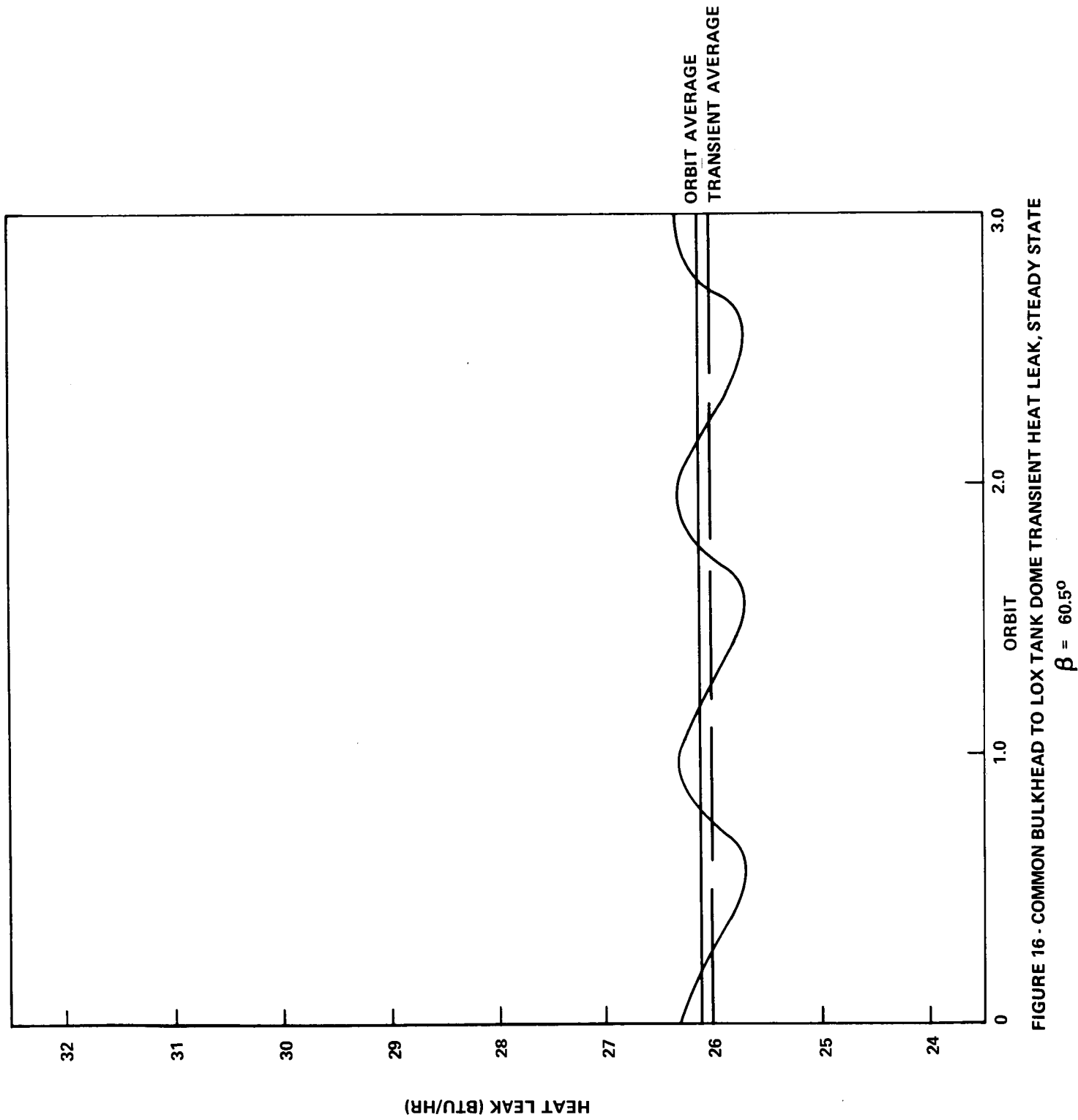
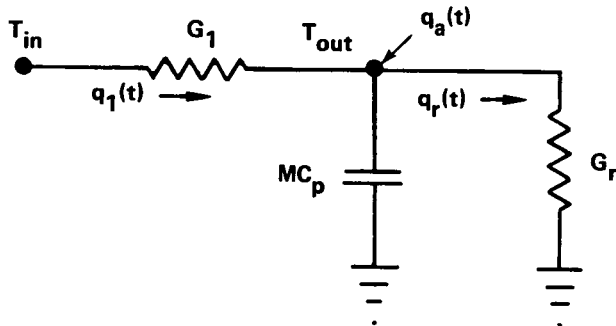


FIGURE 16 - COMMON BULKHEAD TO LOX TANK DOME TRANSIENT HEAT LEAK, STEADY STATE
 $\beta = 60.5^\circ$

APPENDIXEffect of Non-linear Heat Transfer Paths When Interacting with a Transient Thermal Environment

A typical OWS wall section is represented schematically by the following sketch:



T_{in} is the temperature of the inside wall which has a leak component $q_1(t)$ through G_1 . T_{out} is the temperature of the outside wall which has a thermal inertia (capacity) MC_p , absorbs heat $q_a(t)$, and radiates $q_r(t)$ to free space through the radiation conductance G_r . Both G_1 and G_r are non-linear: G_1 , for example, because of internal insulation characteristics in series with possible radiation paths, and G_r because of the customary radiation conductance definition. T_{in} we consider constant and $q_a(t)$, periodic. We would like to note the dependence of $q_1(t)$ on $q_a(t)$ and the network elements.

A heat balance on the outside node gives

$$(1) \quad \sigma \epsilon T_{out}^4(t) + MC_p \frac{dT_{out}(t)}{dt} = q_1(t) + q_a(t)$$

Since $q_1(t) = G_1(T_{in}, T_{out})(T_{in} - T_{out}) = -f(T_{out}, t)$

$$(2) \quad \sigma\epsilon T_{out}^4(t) + f(T_{out}, t) + MC_p \frac{dT_{out}(t)}{dt} = q_a(t)$$

For the OWS, (2) is really a system of equations since there are 96 outside surfaces.

For an isolated, massless surface in free space, $f(T_{out}, t)$ and MC_p are zero. For this case, we get

$$(3) \quad T_{out}(t) = \left[\frac{q_a(t)}{\sigma\epsilon} \right]^{1/4}$$

The orbit-average absorbed heat input is given by

$$(4) \quad \bar{Q} = \frac{1}{P} \int_0^P q_a(t) dt$$

where P is the orbit period. This results in an orbit-average temperature

$$(5) \quad \bar{T}_{out} = \left[\frac{1}{P\sigma\epsilon} \int_0^P q_a(t) dt \right]^{1/4}$$

If however, we elect to find $T_{out}(t)$ before averaging the absorbed heat, then the average per orbit outer temperature is

$$(6) \quad \hat{T}_{out} = \frac{1}{P} \int_0^P T_{out}(t) dt = \frac{1}{P} \left(\frac{1}{\sigma\epsilon} \right)^{1/4} \int_0^P \left[q_a(t) \right]^{1/4} dt$$

Following this line for the 96 OWS surfaces with areas A_i , we have evaluated the heat flux quantities (at $\beta = 60.5^\circ$)

$$(7) \quad \frac{1}{A_i} \left[\frac{1}{P} \int_0^P \left[q_{a_i}(t) \right]^{1/4} dt \right]^4$$

which are compared with

$$(8) \quad \frac{1}{A_i} \left[\frac{1}{P} \int_0^P q_{a_i}(t) dt \right],$$

in Table Al. In all cases, we note that (7) < (8). This implies that the average per-orbit outer surface temperature is less than the orbit average temperature, i.e., $\hat{T}_{out} < \bar{T}_{out}$. Therefore, assuming a reasonably constant inner wall temperature, T_{in} , we would expect to see a bias in the average heat leak components. If we associate \hat{Q}_{LEAK} with \bar{T}_{out} and \hat{Q}_{LEAK} with \hat{T}_{out} , then

$$\hat{Q}_{LEAK} > \bar{Q}_{LEAK}$$

The comparison of the leak components given in Table 6 shows no definite bias. Furthermore, if the OWS model is excited by the flux quantities (7), we obtain heat leaks which are about two times larger than the orbit-average derived leaks. Hence, (2) appears to have been over-simplified by the removal of node capacity and the effect of the internal leak component, $q_1(t)$.

Our next inclination is to evaluate (2) more thoroughly, except that this is exactly what the OWS thermal model accomplishes. Therefore, from the comparison of the leak components in Table 6, we conclude that the effect of non-linear heat transfer paths on heat leak for orbit-average and transient heat input data is negligible.

TABLE A1
COMPARISON OF ORBIT AVERAGE AND TRANSIENT AVERAGE ABSORBED HEATS

	NODES	BOWS (BTU/SEC FT ²)	$\frac{1}{A_i} \left[\frac{P}{P_0} \int_{\infty}^{\infty} [q_{e_i}(t)]^{1/4} dt \right]^4$ (BTU/SEC FT ²)
SOLAR PANELS	501	.08543	.0696488
	502	.08543	.0696488
AIRLOCK SHROUD	1111	.06469	.0472336
	1112	.06375	.0564601
	1113	.06065	.0660125
	1114	.00944	.0040829
INSTRUMENT UNIT	1211	.03936	.0273620
	1212	.08149	.0621458
	1213	.08101	.0671034
	1214	.03755	.0349467
	1215	.00597	.0052946
	1216	.00654	.0062673
	1217	.00840	.0051985
	1218	.00982	.0040495
UPPER FORWARD SKIRT	1311	.03936	.0272988
	1312	.08149	.0619970
	1313	.08101	.0669477
	1314	.03755	.0348701
	1315	.00597	.0052819
	1316	.00654	.0062524
	1317	.00840	.0051864
	1318	.00982	.0040400
LOWER FORWARD SKIRT	1411	.03936	.0272766
	1412	.08149	.0619566
	1413	.08101	.0669058
	1414	.03755	.0348446
	1415	.00597	.0052787
	1416	.00654	.0062479
	1417	.00840	.0051827
	1418	.00982	.0040372
FORWARD METEOROID SHIELD EXTENSION	541	.03936	.0273160
	542	.08149	.0620430
	543	.08101	.0669910
	544	.03755	.0348966
	545	.00597	.0052860
	546	.00654	.0062567
	547	.00840	.0051900
	548	.00982	.0040428
METEOROID SHIELD TOP	510	.03935	.0273061
	511	.03936	.0273423
	512	.08149	.0620713
	513	.08101	.0670218
	514	.03756	.0349114
	515	.00597	.0052920
	516	.00654	.0062532
	517	.00840	.0051922
METEOROID SHIELD BOTTOM	518	.00982	.0040449
	520	.03935	.0273348
	521	.03936	.0273354
	522	.08149	.0620849
	523	.08101	.0670397
	524	.03756	.0349200
	525	.00597	.0052893
	526	.00654	.0062898
AFT METEOROID SHIELD EXTENSION	527	.00840	.0062608
	528	.00982	.0051939
	529	.00982	.0040457
	531	.03936	.0273301
	532	.08149	.0620663
	533	.08101	.0670190
	534	.03756	.0349073
	535	.00597	.0052879
LOWER AFT SKIRT 1	536	.00654	.0062590
	537	.00840	.0051916
	538	.00982	.0040443
	7401	.03936	.0273679
	7402	.08149	.0621612
	7403	.08101	.0621242
	7404	.03756	.0349634
	7405	.00597	.0052962
LOWER AFT SKIRT 2	7406	.00654	.0062686
	7407	.00840	.0051998
	7408	.00982	.0040507
	7201	.01909	.0143180
	7202	.03576	.0301841
	7203	.03593	.0328467
	7204	.01888	.0184904
	7205	.00575	.0048990
IMPINGEMENT CURTAIN	7206	.00578	.0056648
	7207	.00687	.0045573
	7208	.00776	.0034387
	7301	.00795	.0038927
	7302	.00795	.0038927
	7303	.00795	.0038927
	7304	.00795	.0038927
	7305	.00795	.0038927
THRUST CONE	7306	.00795	.0038927
	7307	.00795	.0038927
	7308	.00795	.0038927
	8101	.02621	.0201384
	8102	.05196	.0413141
	8103	.05162	.0436385
	8104	.02497	.0232245
	8105	.00581	.0037671
	8106	.00617	.0043201
	8107	.00728	.0036271
	8108	.00801	.0030475

BELLCOMM, INC.

Subject: Generalization of the Skylab
Orbital Workshop Thermal Model
to Accept Transient External
Absorbed Heat Input Data
Case 620

From: D. P. Woodard
A. W. Zachar

Distribution List

NASA Headquarters

H. Cohen/MLR
J. H. Dishier/MLD
W. B. Evans/MLO
J. P. Field, Jr./MLP
T. E. Hanes/MLA
A. S. Lyman/MR
M. Savage/MLT
W. C. Schneider/ML

Bellcomm

A. P. Boysen
J. P. Downs
D. R. Hagner
W. G. Heffron
J. Z. Menard
P. F. Sennewald
J. W. Timko
M. P. Wilson
Departments 2031, 2034 Supervision
Division 101 Supervision
Division 102
Department 1024 File
Central File
Library

MSC

R. G. Brown/ES-16
C. N. Crews/KS
R. E. Durkee/ES-5
R. L. Frost/KS

ABSTRACT ONLY

I. M. Ross
R. L. Wagner

MSFC

J. M. Boze, Jr./PM-AA-EI
G. B. Hardy/PM-AA-EI
G. D. Hopson/S&E-ASTN-PL
J. W. Littles/S&E-ASTN-PLA
W. C. Patterson/S&E-ASTN-PLA
R. D. Wegrick/S&E-CSE-AA
C. C. Woodard/S&E-ASTN-P